Int. J. Heat Mass Transfer. Vol. 27, No. 9, pp. 1465–1472, 1984
Printed in Great Britain

0017–9310/84 $3.00 + 0.00
© 1984 Pergamon Press Ltd.

Steady-state measurements and analytical correlations of axial effective thermal conductivities in packed beds at low gas flow rates

D. VORTMEYER and W. ADAM

Fakultät für Maschinenwesen, Technische Universität München, 8000 München 2, Arcisstr. 21, Federal Republic of Germany

(*Received* 6 *February* 1984)

Abstract—In agreement with previous authors, effective axial conductivities should be represented as the sum of the effective conductivity without flow and a term which depends on the flow rate. Concerning this latter term it was found in combining our own experimental results with those of Kunii and Smith that the best correlating parameter is the linear artificial velocity rather than the Reynolds number. New correlations for this term are presented which also include gases other than air.

1. INTRODUCTION

THE AXIAL effective heat conductivity λ^e_{ax} without thermal radiation effects is defined by the steady-state quasi-homogeneous model equation of a fixed bed

$$\dot{m}c_f\frac{dT}{dx}-\lambda^e_{ax}\frac{d^2T}{dx^2}=0. \tag{1}$$

Equation (1) is valid only for low flow rates where solid and fluid temperatures are close together. A rather precise knowledge of this effective property is important, e.g. for the analysis of stability phenomena in fixed bed exothermic chemical reactors and for the computation of thermal effects at low flow rates.

A review of literature data and of published correlations for axial conductivities leads to rather confusing results. To our knowledge the first paper to present a correlation for λ^e_{ax} was that of Yagi *et al.* [1]. These authors proposed

$$\frac{\lambda^e_{ax}}{\lambda_f}=\frac{\lambda^e_0}{\lambda_f}+\delta\ Re\ Pr \tag{2}$$

with $\delta = 0.8$ and 0.7 for glass beads and steel balls, respectively. It is observed that λ^e_{ax}/λ_f is the sum of the dimensionless fixed bed effective conductivity λ^e_0/λ_f without flow and of a contribution which depends on the Reynolds and Prandtl numbers. Since the coefficient δ in equation (2) is similar for beds of steel and glass particles we conclude that the term $\delta\ Re\ Pr$ is practically independent of the heat conductivity of the solid material. Shortly after the work of Yagi *et al.* [1], Kunii and Smith [2] published data on the same topic. Their measurements for glass beads and sand particles show that the flow contribution in equation (1) is not linear in Reynolds number and is affected strongly by the particle diameter. They also varied the type of gas. However, beyond a graphical presentation Kunii and Smith did not offer an analytical correlation.

Votruba *et al.* [3] published steady-state data and found the flow-dependent contribution in equation (2) to be a function of Re, d_p and a constant C which is specific for each experimental run and which therefore has to be taken from Table 1 of their paper. They proposed the expression

$$\frac{\lambda^e_{ax}}{\lambda_f}=\frac{\lambda^e_0}{\lambda_f}+\frac{14.5}{d_p(1+C/Re\ Pr)}. \tag{3}$$

For numerical calculation d_p is in mm.

After reviewing the available experimental material with the exception of ref. [2], Dixon and Cresswell [4] concluded that the correlation should be

$$\frac{\lambda^e_{ax}}{\lambda_f}=\frac{\lambda^e_0}{\lambda_f}+\frac{0.5}{1+\varepsilon\beta/Re\ Pr} \tag{4}$$

where ε is the relative voidage (porosity) of the packed bed and β is a constant which is equal to 9.7 for air. They also included dispersion data obtained by Gunn and de Souza [5] for unsteady heat dispersion and dispersion data by Edwards and Richardson [6] for unsteady mass dispersion. Dietrich [7] derived from his experimental work on ignition and extinction of chemical packed bed reactors that for his catalyst, Al_2O_3 particles ($d_p = 6$ mm), the coefficient δ in equation (2) should be equal to 0.3 instead of 0.7 or 0.8 as in ref. [1].

To conclude this survey we find agreement between all authors that the effective thermal conductivity consists of the effective conductivity λ^e_0 without flow and a contribution depending on the flow rate. It is the latter term on which large differences are observed. The order of disagreement is presented in Figs. 1 and 2 where the flow-dependent contribution

$$\lambda^e_{ax}/\lambda_f-\lambda^e_0/\lambda_f=F \tag{5}$$

was evaluated from available correlations and experimental results for glass and steel particles. Some of our own measurements are also included. None of the available correlations describe correctly what is observed from experiments. This statement applies in particular to the strong sensitivity of F with respect to d_p if F is plotted as a function of Reynolds number.

NOMENCLATURE

a_N	thermal diffusivity at 273 K [$m^2 s^{-1}$]
c_f	heat capacity of fluid [$J kg^{-1} K^{-1}$]
d_p	particle diameter [m]
D	packed bed diameter [m]
F	$\lambda^e_{ax}/\lambda_f - \lambda^e_0/\lambda_f$, equation (5)
K	coefficient in equation (19)
$\dot{m}$	specific mass flux [$kg m^{-2} s^{-1}$]
Pr	ν_N/a_N at 273 K
Re	$\dot{m}d_p/\nu_N$ at 273 K
T	temperature [K]
T_0	temperature of the heated surface [K]
T_u	surrounding temperature [K]
u_N	linear artificial velocity (plug flow) at 273 K [$m s^{-1}$]
x	coordinate
$Z_{1,2}$	equation (15).

Greek symbols

α_w	overall wall heat transfer coefficient [$J m^{-2} s^{-1} K^{-1}$]
λ^e_{ax}	effective axial heat conductivity of a packed bed with flow [$J m^{-1} s^{-1} K^{-1}$]
λ^e_0	effective heat conductivity of a packed bed without flow [$J m^{-1} s^{-1} K^{-1}$]
λ_f, λ_s	heat conductivities of fluid and solid [$J m^{-1} s^{-1} K^{-1}$]
ν_N	viscosity at 273 K [$m^2 s^{-1}$]
χ, χ_v, χ_{ad}	equations (9), (12), (14) and (15) [m^{-1}].

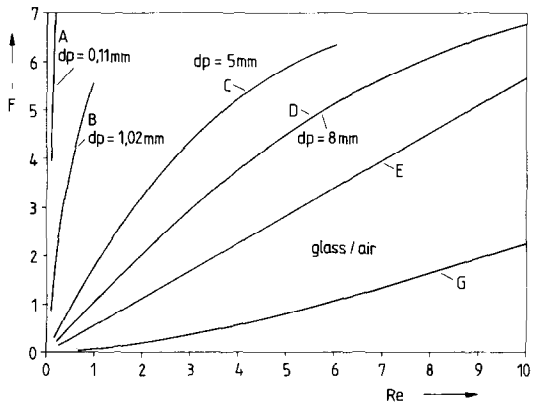

FIG. 1. $\lambda^e_{ax}/\lambda_f - \lambda^e_0/\lambda_f = F$ as a function of Re for the glass–air system: A, B, Kunii and Smith [2]; C, D, present results; E, Yagi *et al.* [1], equation (2); G, Dixon and Cresswell [4], equation (4).

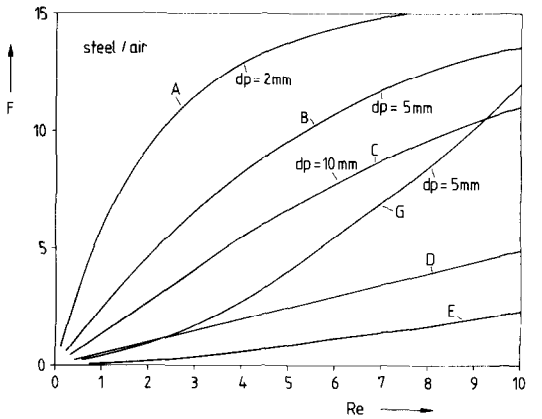

FIG. 2. $F = f(Re)$ for the steel–air system: A, B, C, present results; D, Yagi *et al.* [1], equation (2); E, Dixon and Cresswell [4], equation (4); G, Votruba *et al.* [3], equation (3).

2. EXPERIMENTAL AND THEORETICAL BACKGROUND

If heat is supplied by thermal radiation or by other means to the exit cross-section of a fixed bed with a gas-stream through it, heat conduction against the fluid flow gives rise to temperature profiles (Fig. 3). This method was first employed by Saunders *et al.* [8] for the determination of heat transfer coefficients in porous metallic walls. Certainly this experimental technique is restricted to low flow rates because at higher rates convective processes dominate so that heat conduction against flow is very small and profiles like those in Fig. 3 are no longer observed.

It is the equilibrium between conduction and convection in each cross-section which determines the length of the temperature profile as a function of flow rate. Since the effective quiescent conductivity λ^e_0 of a packed bed depends on the conductivity λ_s of the solid material it is expected that this solid conductivity should also influence the outcome of the experiments.

We adopted for our measurements the method of Saunders *et al.* [8] as previous authors before [1–3]. Since the smallest diameter of the spherical particles was 2 mm we decided to measure temperatures by fitting thermocouples within particles which were positioned on the centerline of the circular packed bed. For a control radial profiles were measured in several cross-sections.

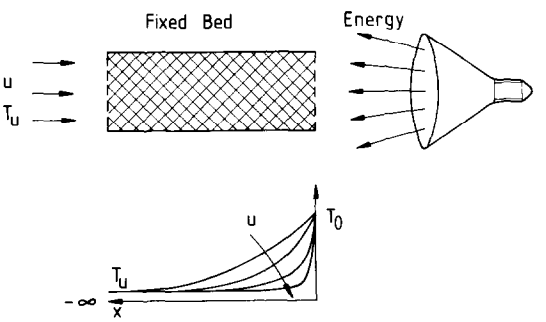

FIG. 3. General survey.

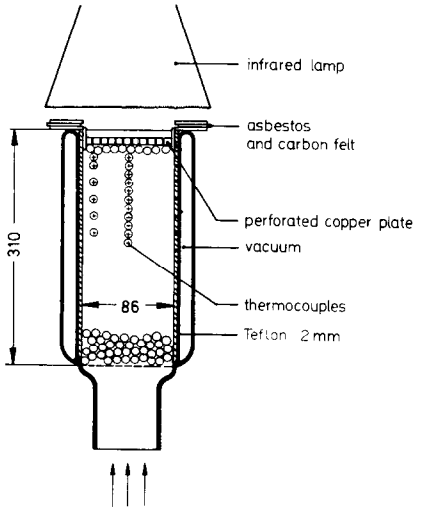

FIG. 4. The containers for spherical particles.

Vessels with different internal diameters of 86, 139 and 200 mm were used as containers for the particles. The 86 mm vessel was a Dewar flask, the others were made of stainless steel with a wall thickness of 0.3 mm. They were surrounded by fibre filled evacuated jackets with an outside thermal insulation. In order to minimize the effect of axial heat conduction inside the glass and metallic walls, a circular cylinder of Teflon with a wall thickness of 2 mm was placed between the spherical particles and the wall (Fig. 4). Heat was supplied from an infrared lamp to a perforated copper plate on top of the fixed bed. The copper plate secured constant temperatures across the bed exit. The experiments were conducted with spherical particles of low thermal conductivity as the catalyst support material Al_2O_3 or plastic, with glass spheres of moderate and metal spheres (steel, bronze, brass) of high thermal conductivity. All experiments were performed with air. The inlet temperature of the gas and the room temperature was kept constant. The experimental task was to measure a large number of axial temperature profiles (Fig. 3) as a function of flow velocity.

Although the insulation of the experimental vessel was good and radial temperature profiles were flat, particularly at low flow rates, radial heat losses could not be avoided. Therefore, Gunn [9] took account of these losses by adding an overall heat loss term to the quasi-homogeneous model equation (1). Instead of equation (1) we then have

$$\dot{m}c_f\frac{dT}{dx}-\lambda_{ax}^e\frac{d^2T}{dx^2}+\frac{4\alpha_w}{D}(T-T_u)=0 \qquad (6)$$

where T_u is the temperature of the surroundings. α_w is assumed to be independent of the flow velocity. The solution of equation (6) with respect to the boundary conditions (Fig. 2)

$$\begin{aligned} x&=0, \quad T=T_0\\ x&\to-\infty, \quad T=T_u \end{aligned} \qquad (7)$$

is given by the expression

$$\frac{T-T_u}{T_0-T_u}=\exp\left\{x\left[\frac{\dot{m}c_f}{2\lambda_{ax}^e}+\sqrt{\left[\left(\frac{\dot{m}c_f}{2\lambda_{ax}^e}\right)^2+\frac{4\alpha_w}{D\lambda_{ax}^e}\right]}\right]\right\} \qquad (8)$$

for $x<0$ as in Fig. 3 or in terms of Re and Pr

$$\frac{T-T_u}{T_0-T_u}=\exp\left\{x\left[\frac{Re\,Pr}{2d_p(\lambda_{ax}^e/\lambda_f)}+\sqrt{\left[\left(\frac{Re\,Pr}{2d_p(\lambda_{ax}^e/\lambda_f)}\right)^2+\frac{4\alpha_w}{D\lambda_{ax}^e}\right]}\right]\right\}=\exp(x\chi_v) \qquad (9)$$

with

$$\chi_v=\frac{Re\,Pr}{2d_p(\lambda_{ax}^e/\lambda_f)}+\sqrt{\left[\left(\frac{Re\,Pr}{2d_p(\lambda_{ax}^e/\lambda_f)}\right)^2+\frac{4\alpha_w}{D\lambda_{ax}^e}\right]}. \qquad (10)$$

With respect to λ_{ax}^e we obtain from equation (10)

$$\frac{\lambda_{ax}^e}{\lambda_f}=\frac{Re\,Pr}{\chi_v d_p}+\frac{1}{\chi_v^2}\frac{4\alpha_w}{\lambda_0^e D}. \qquad (11)$$

Equation (9) reduces for $\alpha_w=0$ to the well-known adiabatic equation from refs. [1–3]

$$\begin{aligned}\frac{T-T_u}{T_0-T_u}&=\exp\left(x\frac{\dot{m}_f c_f}{\lambda_{ax}^e}\right)\\&=\exp\left(x\frac{Re\,Pr}{d_p(\lambda_{ax}^e/\lambda_f)}\right)\\&=\exp(x\chi_{ad})\end{aligned} \qquad (12)$$

and

$$\frac{\lambda_{ax}^e}{\lambda_f}=\frac{Re\,Pr}{d_p\chi_{ad}}. \qquad (13)$$

Both equations (9) and (12) are represented by a straight line in the plot

$$\ln\left(\frac{T-T_u}{T_0-T_u}\right)=x\chi \qquad (14)$$

with a slope of χ_v or χ_{ad} respectively. Not one of our measurements turned out to fulfil adiabatic conditions.

3. EXPERIMENTAL RESULTS AND THE EVALUATION OF AXIAL EFFECTIVE CONDUCTIVITIES

In fact if the actually measured temperature profiles were plotted in the way suggested by equation (14), like other authors before we also obtained straight lines which substantiate the concept of an axial effective conductivity. Figure 5 is representative of several hundred measured profiles. The slope χ_v is easily evaluated for each profile. Since the slope depends on the flow rate it was plotted as a function of Reynolds number. Figures 6 and 7 only serve as examples for many more similar plots under different experimental conditions. Each point in Figs. 6 and 7 corresponds with a measured temperature profile.

In all cases the χ_v-functions were found to be straight lines, e.g. (Figs. 6 and 7) in the low Reynolds number

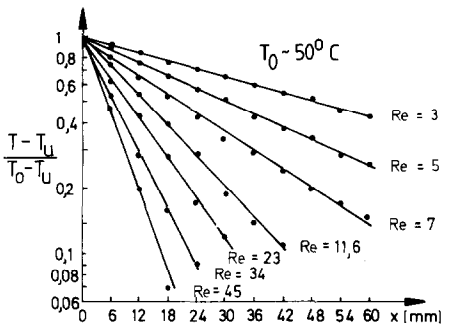

FIG. 5. Semi-logarithmic plot of measured temperature profiles vs χ.

range. These lines were extended to the point of intersection with the ordinate. The ordinate sections are a measure of the heat losses since under adiabatic conditions χ should be zero for $Re = 0$. The linear range of χ_v is represented by the function

$$\chi_v = Z_1 + Re\ Z_2. \tag{15}$$

Table 1 contains numerical values of Z_1 and Z_2 under different experimental conditions. It is observed that Z_1 which is a measure for the heat losses, generally decreases with increasing diameter D of the particle bed, a fact which was expected.

By a comparison of equations (15) and (10) we find at $Re = 0$ and $\lambda^e_{ax} \to \lambda^e_0$

$$Z_1 = \sqrt{\left(\frac{4\alpha_w}{\lambda^e_0 D}\right)}. \tag{16}$$

Therefore, equation (11) can be rewritten as

$$\frac{\lambda^e_{ax}}{\lambda_f} = \frac{Re\ Pr}{\chi_v d_p} + \frac{Z_1^2}{\chi_v^2}\frac{\lambda^e_0}{\lambda_f}. \tag{17}$$

At this stage the effective conductivities λ^e_{ax}/λ_f could be evaluated from equation (17) if numerical values for (λ^e_0/λ_f) were estimated from correlations [10–12] or graphical mappings [13] which are available in the literature. However, it will be shown that (λ^e_0/λ_f)-values are also obtainable from the experimental results of this paper.

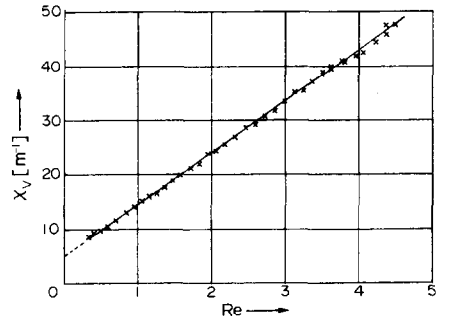

FIG. 6. $\chi_v = f(Re)$ for 5 mm spherical glass particles, No. 7 of Table 1.

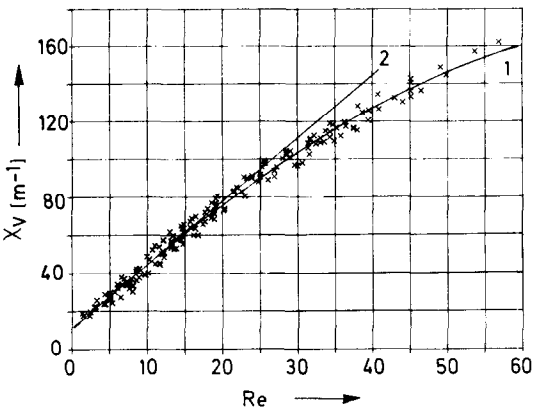

FIG. 7. $\chi_v = f(Re)$ for 6 mm steel spheres, No. 18 of Table 1. 2, straight line approximation for low Re numbers.

The first derivative of equation (10) with respect to Re is at $Re = 0$

$$\left(\frac{d\chi_v}{d\ Re}\right)_{Re=0} = \frac{1}{2d_p(\lambda^e_0/\lambda_f)}\left[Pr - Kd_p\sqrt{\left(\frac{4\alpha_w}{D\lambda_f(\lambda^e_0/\lambda_f)}\right)}\right]. \tag{18}$$

In order to obtain equation (18) it was assumed that $(\lambda^e_{ax}/\lambda_f)$ can be represented by a functional relation of the type

$$\frac{\lambda^e_{ax}}{\lambda_f} = \frac{\lambda^e_0}{\lambda_f} + \frac{K\ Re}{1 + C\ Re} \tag{19}$$

with $C = 0$ or $C \neq 0$ as suggested by available literature data. It is further observed from equation (15) that

$$\left(\frac{d\chi_v}{d\ Re}\right)_{Re=0} = Z_2. \tag{20}$$

Equations (20) and (16) allow us to rewrite equation (18) in terms of Z_1 and Z_2

$$\frac{\lambda^e_0}{\lambda_f} = \frac{1}{2d_p Z_2}(Pr - Kd_p Z_1). \tag{21}$$

Since the second term within the parentheses of equation (21) is a relatively small correction term, as a first step λ^e_0/λ_f is evaluated from equation (21) by neglecting this term. Consecutive values for $(\lambda^e_{ax}/\lambda_f)$ are estimated from equation (17) with the data of Table 1. The coefficient K [equation (19)] is obtained from a plot

$$\frac{\lambda^e_{ax}}{\lambda_f} - \frac{\lambda^e_0}{\lambda_f} = F = f(Re). \tag{22}$$

With K known we evaluate corrected data of λ^e_0/λ_f from equation (21). This procedure which can be repeated if necessary, was applied to each of the 22 different experimental cases in Table 1. The table includes the averaged values of λ^e_0/λ_f for each material.

A comparison of these data in Table 2 with predictions of the correlations [9, 10] turns out to be quite satisfactory.

For the final calculations of F however the individual (λ^e_0/λ_f)-data were used and not the averaged.

Table 1. Experimental details

No.	Material	λ_s/λ_f	$d_p \times 10^3$ (m)	$D \times 10^3$ (m)	D/d	Re	Z_1 (m^{-1})	Z_2 (m^{-1})	λ_0^e/λ_f	$\overline{\lambda_0^e/\lambda_F}$
1	Catalyst	~ 4.1	5	86	17.2	0.1– 6.0	20.0	17.5	3.5	4
2			6	86	14.33	1.5– 3.5	23.5	11.5	4.4	
3	Polyamid	~ 8.2	6	86	14.33	1.5– 4.0	20.0	9.9	4.7	4.6
4			6	139	23.2	1.5– 6.0	13.5	11.3	4.5	
5	Glass	45	5	86	17.2	0.1– 6.0	16.0	7.65	7.9	
6			5	139	27.8	0.1– 6.0	11.3	9.0	7.1	
7			5	200	40.0	0.3– 3.0	5.0	9.52	—	7.9
8			8	86	10.75	2 –12.0	17.0	4.3	8.7	
9			8	139	17.4	1.5– 8.5	10.5	5.0	8.0	
10	Bronze	850	6	86	14.33	1.5– 9.5	9.5	3.35	14.3	14.3
11	Brass	1660	6	86	14.33	1.5– 9.0	10.0	2.9	16.6	16.6
12	Steel	1470	2	86	43.0	1.3– 6.3	10.0	10.9	14.5	
13			2.5	86	34.4	1.0– 7.0	12.3	9.23	13.3	
14			3	205	68.33	0.4– 1.2	1.5	7.62	—	15.1
15			3.5	86	24.6	0.1–12.0	11.5	5.73	15.4	
16			4	86	21.5	1.0–12.0	17.0	4.8	15	
17			5	86	17.2	1.0–13.0	12.0	3.8	16.2	
18			6	86	14.33	1.0–12.5	11.7	3.35	15.3	
19			6	139	23.2	1.5– 8.0	4.0	3.73	—	
20			6	200	33.3	1.0–11.0	2.0	4.05	—	
21			10	86	8.6	2.0–20.0	8.7	1.9	16.9	
22			10	139	13.9	1.5–11.0	8.5	2.1	15.3	

Figures 1 and 2 incorporate our own data of F for steel and glass spheres as a function of Reynolds number. In agreement with Kunii and Smith [2] these data also depend on the particle diameter. In fact Fig. 2 for the glass–air system shows nicely the extension of Kunii and Smith's data for small glass particles to the situation where the diameters are 5 and 8 mm as in our experiments.

It has to be concluded from these results that the Reynolds number obviously is not a suitable correlating parameter. This is understandable on the grounds that the particle diameter should not have a particular meaning in a true quasi-homogeneous medium. In fact the original solutions, equations (8) and (12), of the quasi-homogeneous equations do not contain the particle diameter at all. It is only introduced artificially if the solutions, equations (8) and (12), are expressed in terms of the dimensionless Reynolds and Prandtl numbers.

The situation changes completely if F is plotted as a function of the artificial linear velocity u_N which here is related to 273 K. The dramatic impact of the change of variable is particularly demonstrated by Fig. 8 which besides our own results for particle diameters of 8 and 5 mm also contains those of Kunii and Smith with particle diameters between 0.11 and 1.02 mm. Within small scatter all data lie practically on one line. Similar plots for steel, brass and bronze particles and for catalyst and polyamid spheres are presented in Figs. 9 and 10.

Although there is some scatter for metal spheres, nevertheless the bulk of the measurements is quite close together. The scatter may reflect partly the influence of the ratio D/d_p, although no definite conclusions could be drawn.

Furthermore, it is observed that the F-functions depend also on the heat conductivities λ_s of the solid material. The lines in Figs. 8–10 are overall analytically

Table 2. Measured and calculated data of λ_0^e/λ_f

Material	λ_s/λ_f	λ_0^e/λ_f measured	λ_0^e/λ_f after [11]	λ_0^e/λ_f after [10]
Catalyst	~ 4	3.9	2.2	2.2
Polyamid	~ 8	4.6	3.3	3.0
Glass	45	7.9	6.8	6.4
Bronze	—	14.3	—	—
Brass	1660	16.6	17	18.5
Steel	1470	15.2	16.6	18.5

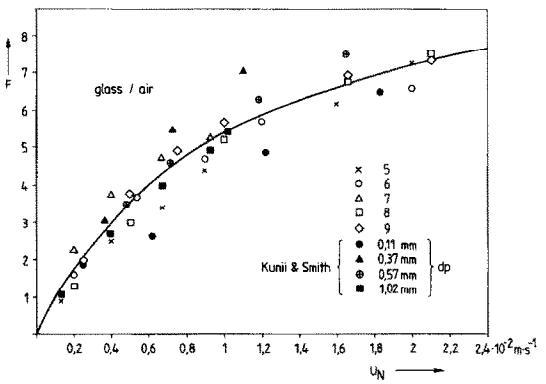

FIG. 8. $F = f(u_N)$ for the glass–air system. Numbers 5–9 of Table 1.

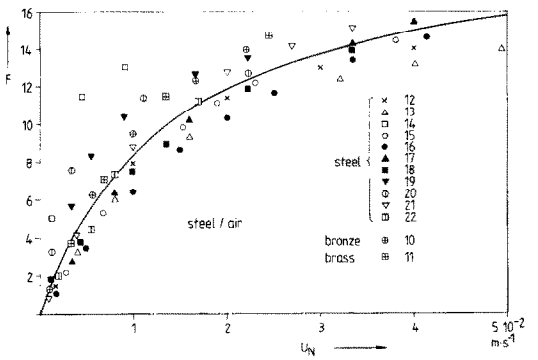

FIG. 9. $F = f(u_N)$ for metal–air system. Numbers 10–22 of Table 1.

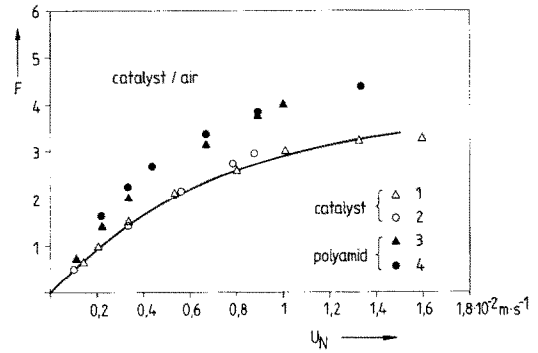

FIG. 10. $F = f(u_N)$ for catalyst support Al_2O_3–air and polyamid–air systems. Numbers 1–4 of Table 1.

fitted by the relation

$$F = \frac{gu_N}{1 + hu_N} \tag{23}$$

or

$$\frac{\lambda^e_{ax}}{\lambda_f} = \frac{\lambda^e_0}{\lambda_f} + \frac{gu_N}{1 + hu_N} \tag{24}$$

or

$$\frac{\lambda^e_{ax}}{\lambda_f} = \frac{\lambda^e_0}{\lambda_f} + \frac{gv_N\, Re/d_p}{1 + hv_N\, Re/d_p} \tag{25}$$

with d_p in m and v_N in $m^2\,s^{-1}$. Table 3 lists g and h for the metal–air, glass–air and catalyst support–air systems. Either equation (24) or equation (25) may be used for the evaluation of effective conductivities at low flow rates.

Table 3. Coefficients g and h of equation (24) for air only

System	g (m^{-1} s)	h (m^{-1} s)
Metal–air	14.2×10^2	0.7×10^2
Glass–air	10.6×10^2	0.96×10^2
Catalyst–air	6×10^2	1.1×10^2

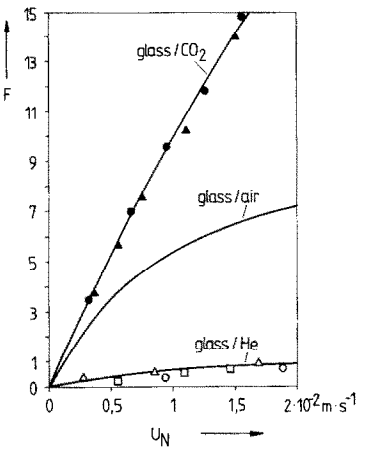

FIG. 11. $F = f(u_N)$ glass–CO_2, glass–air and glass–He systems.

4. THE EFFECT OF DIFFERENT GASES

Besides air Kunii and Smith [2] also performed experimental work with helium and carbon dioxide flowing through packed beds of glass beads. The effect on F is very large as exhibited by Fig. 11 which contains some of their results for CO_2 and He. The glass–air system is represented by the calculated curve from equation (24). A reduction of the three different curves in Fig. 11 to one is obtained if F is multiplied by the thermal diffusivities $a_N = (\lambda_f/\rho c_p)_N$ of the different gases. Numerical values at 273.15 K are: $a_{N,CO_2} = 0.0887 \times 10^{-4}$; $a_{N,air} = 0.173 \times 10^{-4}$ and $a_{N,He} = 1.53 \times 10^{-4}\ m^2\,s^{-1}$.

Table 4 shows the calculated figures. At constant u_N it is noted that Fa_N is practically the same for each gas. The averaged Fa_N values of Table 4 are plotted in Fig. 12 against the linear velocity u_N. The corresponding analytical expression was found to be

$$Fa_N = \frac{ku_N}{1 + pu_N} \tag{26}$$

or

$$F = \frac{1}{a_N} \frac{ku_N}{1 + pu_N}. \tag{27}$$

Table 4. Reduction of F by the thermal diffusivity a_N

Gas	$u_N \times 10^2$ ($m\,s^{-1}$)	F	$Fa_N \times 10^4$ ($m^2\,s^{-1}$)	$\overline{Fa_N} \times 10^4$ ($m^2\,s^{-1}$)
CO_2		5	0.44	
Air	0.5	3.5	0.61	0.5
He		0.3	0.46	
CO_2		9.5	0.84	
Air	1	5.5	0.95	0.91
He		0.6	0.93	
CO_2		14	1.24	
Air	1.5	6.5	1.12	1.2
He		0.8	1.23	
CO_2		—		
Air	2.0	7.3	1.26	1.4
He		1	1.54	

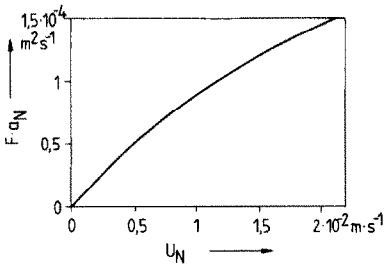

FIG. 12. The reduction of Fig. 11 by $Fa_N = f(u_N)$.

We obtain with F from equation (5)

$$\frac{\lambda_{ax}^e}{\lambda_f} = \frac{\lambda_0^e}{\lambda_f} + \frac{1}{a_N}\frac{ku_N}{1+pu_N} \tag{28}$$

or in terms of Re and Pr

$$\frac{\lambda_{ax}}{\lambda_f} = \frac{\lambda_0^e}{\lambda_f} + \frac{k\ Pr\ Re/d_p}{1+v_N p\ Re/d_p} \tag{29}$$

with d_p is in m and v_N in $m^2\ s^{-1}$.

Equation (29) is valid for packed beds of glass spheres and any gases.

The same procedure was applied to the F-values for metal and catalyst particles although so far experimental evidence is only available for air as the gas flowing through the packed bed. The results are expressed analytically by equations similar to equation (28) or equation (29), however with different numbers for k and p which are presented for all three cases in Table 4.

This extension to other gases is considered to be very important because now a way is open to calculate axial effective conductivities of packed beds with low linear velocities quite generally since coefficients are available for packed beds consisting of solid materials with quite different solid thermal conductivities λ_s.

5. CONCLUSIONS

In agreement with previous work, the axial effective thermal conductivity of a packed bed with gas flow should be presented as the sum of the effective conductivity of the bed without flow and a term which depends on the flow rate. Concerning the latter term it was found conclusively by a combination of our own experimental work and the published data of Kunii and Smith [2] that this term does not correlate with the Reynolds number Re only. The particle diameter is a very important parameter in such correlations.

Table 5. Coefficients k and p of equation (28) for all gases

Material	k (m^{-1} s)	p (m^{-1} s)
Metal	0.026	75
Glass	0.011	25
Catalyst support	0.0088	79.6

Best correlations were obtained by plotting the flow-dependent contribution as a function of the linear artificial flow velocity. Having perceived this fact it was possible to develop new analytical expressions for the metal–air, glass–air and catalyst support–air systems. A still further generalization including gases other than air was obtained by taking into consideration the thermal diffusivities of those gases.

Obviously the particle diameter is not a characteristic length of the system at low flow rates. This result may explain why Saunders *et al.* [8] found the Nusselt number to depend on the particle diameter if Nu was plotted as a function of the Reynolds number for low flow rates in porous materials.

REFERENCES

1. S. Yagi, D. Kunii and N. Wakao, Studies on axial effective thermal conductivities in packed beds, *A.I.Ch.E. Jl* **6**, 543 (1960).
2. D. Kunii and J. M. Smith, Heat transfer characteristics of porous rocks, Part II, *A.I.Ch.E. Jl* **7**, 29 (1961).
3. J. Votruba, V. Hlavacék and M. Marek, Packed bed axial thermal conductivity, *Chem. Engng Sci.* **27**, 1845 (1972).
4. A. Dixon and D. L. Cresswell, Theoretical prediction of effective heat transfer parameters in packed beds, *A.I.Ch.E. Jl* **25**(4), 663 (1979).
5. D. J. Gunn and J. F. C. de Souza, Heat transfer and axial dispersion in packed beds, *Chem. Engng Sci.* **29**, 1363–1371 (1974).
6. M. F. Edwards and J. F. Richardson, Gas dispersion in packed beds, *Chem. Engng Sci.* **23**, 109 (1968).
7. K. Dietrich, Der Festbettreaktor mit exothermer Reaktion im Experiment und mathematischen Modell, TU München, Fakultät Maschinenwesen und Elektrotechnik, Diss. (1972).
8. P. Grootenhuis, R. C. A. Mackworth and O. A. Saunders, Heat transfer of air passing through heated porous metals, *Proc. Instn Mech. Engrs* 363 (1951).
9. D. J. Gunn, Private communication (1982).
10. R. Krupiczka, Analysis of thermal conductivity in granular materials, *Int. Chem. Engng* **7**, 122 (1967).
11. P. Zehner and E. U. Schlünder, Wärmeleitfähigkeit von Schüttungen bei mäßigen Temperaturen, *Chemie–Ingr–Tech.* **42**, 933 (1970).
12. D. Kunii and J. M. Smith, Heat transfer characteristics of porous rocks, Part I, *A.I.Ch.E. Jl* **6**, 71 (1960).
13. N. Wakao and K. J. Kato, Effective thermal conductivity of packed beds, *Chem. Engng Japan* **2**, 24 (1969).

MESURES D'ETAT STATIONNAIRE ET FORMULATION ANALYTIQUE DE CONDUCTIVITES THERMIQUES EFFECTIVES AXIALES DANS DES LITS FIXES A FAIBLE DEBIT DE GAZ

Résumé—En accord avec de précédents auteurs, les conductivités effectives axiales peuvent être représentées comme la somme de la conductivité, effective sans écoulement et d'un terme qui dépend de l'écoulement. En ce qui concerne ce dernier terme, on trouve en combinant les résultats expérimentaux présents avec ceux de Kunii et Smith que le meilleur paramètre d'adaptation est la vitesse linéaire fictive plutôt que le nombre de Reynolds. De nouvelles formulations de ce terme sont présentées qui incluent aussi d'autres gaz que l'air.

MESSUNG UND KORRELATION DER AXIALEN EFFEKTIVEN WÄRMELEITFÄHIGKEIT VON FESTBETTEN BEI GERINGER GASSTRÖMUNG IM STATIONÄREN ZUSTAND

Zusammenfassung—In Übereinstimmung mit früheren Autoren ist die axiale effektive Wärmeleitfähigkeit einer durchströmten Schüttung als Summe aus der effektiven Ruheleitfähigkeit und einem von der Strömungsgeschwindigkeit abhängigen Term darstellbar. Im Hindblick auf diesen zweiten Term führten eigene Meßergebnisse in Kombination mit jenen von Kunii und Smith zu dem Ergebnis, daß eine Korrelation dieses Termes allein mit der Reynoldszahl nicht möglich ist. Der richtige Korrelationsparameter ist die auf den freien Querschnitt bezogene lineare Gasgeschwindigkeit. Auf dieser Grundlage wurden neue Korrelationen entwickelt, die auch den Effekt anderer Gase als Luft mit einschließen.

СТАЦИОНАРНЫЕ МЕТОДЫ ИЗМЕРЕНИЯ И АНАЛИТИЧЕСКИЕ ЗАВИСИМОСТИ ДЛЯ ОПРЕДЕЛЕНИЯ АКСИАЛЬНОЙ ЭФФЕКТИВНОЙ ТЕПЛОПРОВОДНОСТИ ПЛОТНЫХ СЛОЕВ ПРИ НИЗКИХ СКОРОСТЯХ ТЕЧЕНИЯ ГАЗА

Аннотация—Согласно опубликованным в литературе данным коэффициент эффективной осевой теплопроводности выражается в виде суммы эффективной теплопроводности при отсутствии течения и слагаемого, зависящего от скорости течения. При рассмотрении полученных в настоящей работе экспериментальных данных и результатов, полученных Кунии и Смитом, показано, что в этом слагаемом следует использовать не число Рейнольдса, а искусственное значение линейной скорости. Представлены новые зависимости для расчета такого слагаемого, которые можно использовать и для других, отличных от воздуха, газов.